Technical Report

Development of High-strength Nitriding Steel for Next-generation Gears

Takahide UMEHARA* Masato YUYA
Makoto EGASHIRA

Abstract

The electrification of automotive powertrains is expected to advance further; however, gear components such as reduction gears and differentials remain essential for e-Axles, as in conventional gasoline vehicles. In addition to achieving high strength for compact and lightweight designs, reducing CO_2 emissions during manufacturing is critical from an environmental perspective. Nitriding, a thermochemical surface-hardening process, offers smaller heat-treatment distortion and superior dimensional accuracy compared with the currently prevalent carburizing and quenching, enabling simplification or elimination of post-grinding operations. Conversely, the fatigue strength of nitrided components tends to be lower. This paper therefore introduces case studies of research and development at Nippon Steel Corporation aimed at enhancing the strength of nitrided components to broaden their applicability to gears.

1. Introduction

The automotive industry is experiencing a trend toward electrification, and the market share of gasoline vehicles, currently dominant, is expected to decline.[1)] Nevertheless, even in electric vehicles (EVs), i.e., e-Axles replacing engines, reduction gear sets and differentials are still required, and gear components will therefore continue to play important roles. Since improving driving efficiency (electric power consumption) is a common challenge across electrified vehicles (xEVs), gears are required to be high-strength to enable compactness and lightweighting. Furthermore, life-cycle assessment (LCA) aimed at lowering environmental impact is being emphasized more than ever; therefore, efforts to reduce CO_2 emissions through process simplification are expected to become essential.

Figure 1 schematically illustrates representative damage modes of gears. Gears transmit the driving force of engines or motors to the wheels and, under repeated sliding, (i) the tooth root, an area of stress concentration, may fracture due to bending fatigue, and (ii) pits may form at depths of several hundred micrometers (μm) below the tooth-flank contact surface (pitting). To prevent these fatigue damages, gears are usually subjected to surface-hardening heat treatments; at present, the vast majority employ carburizing and quenching. **Figure 2**(a) shows a calculated Fe-C binary phase diagram. Because carburizing and quenching are high-temperature treatments at ≥900°C, they provide a deep hardened layer and excellent fatigue strength. However, quenching causes large distortion; therefore, grinding is required to ensure low noise. Accordingly, nitriding has attracted increasing attention because it offers superior noise performance of components compared with carburizing. In contrast, nitriding is performed in the ferrite (α) region of the Fe-N binary system at 500–600°C without phase transformation, and thus

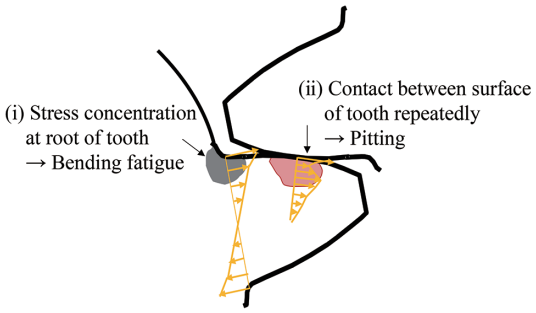

Fig. 1 Typical damage patterns of gears

* Senior Manager, Head of Section, Integrated Steel-Solution Research Lab.-II, Steel Research Laboratories
20-1 Shintomi, Futtsu City, Chiba Pref. 293-8511

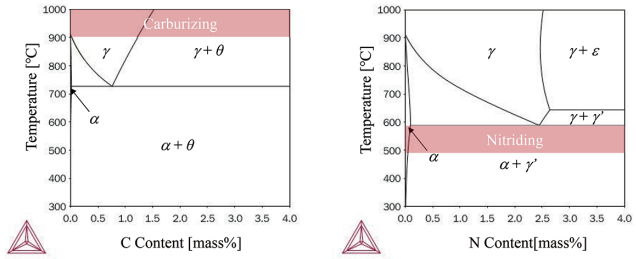

(a) Fe-C binary alloy system (b) Fe-N binary alloy system

Fig. 2 Calculated phase diagrams (a) Fe-C and (b) Fe-N binary alloy system (Thermo-Calc2020, SSOL ver.5)

features smaller distortion than carburized parts and allows simplification of post-grinding. Therefore, nitriding is suitable for thin-walled gear components and for components requiring high dimensional accuracy. On the other hand, for gear applications, the hardened layer is shallower than that produced by carburizing and quenching due to the difference in treatment temperatures; in addition, the influence of the nitrogen compound layer described in the next chapter tends to lower tooth-root bending fatigue and pitting strength. Consequently, application of nitriding is often limited to parts subjected to relatively low stresses, and increasing the strength of nitrided parts is regarded as a major issue for expanding the scope of application.

Against this background, we introduce our research and development (R&D) cases aimed at expanding the application of nitriding to gear components by increasing the strength of nitrided parts.

2. Characteristics of Hardened Layers Formed by Gas Nitriding

Figure 3 shows micrographs of the surface-region cross section and a schematic hardness profile of nitrided steel. Nitriding of steel produces a matrix strengthened by dissolved nitrogen and precipitated nitrides (diffusion layer) and, at the topmost surface, forms a compound layer composed of iron nitrides with a thickness of approximately 10–20 μm.[2)]

Regarding modification of the diffusion layer, numerous studies have been reported; it is widely recognized that alloying elements influence the hardening characteristics of the diffusion layer. In particular, when alloying elements such as Cr that readily form compounds with nitrogen are present in steel, increasing their content leads to increased hardening of the nitrided layer.[3–5)]

The compound layer formed directly above the diffusion layer mainly contains two phases: the hard and brittle ε-phase ($Fe_{2\sim3}N$) and the softer but more deformable γ'-phase (Fe_4N). Under general gas-nitriding conditions, the compound layer is typically ε single phase, has lower deformability than the matrix, and often exhibits a porous layer at the very surface;[2)] consequently, in pitting and tooth-root bending fatigue, cracks and delamination readily occur and act as fracture origins.[6, 7)] In recent years, as sensors for controlling the nitriding atmosphere have become widespread, efforts to improve fatigue strength by modifying the compound layer have become increasingly common,[8–10)] and Nippon Steel Corporation has introduced nitriding furnaces with controllable atmospheres for the same purpose.

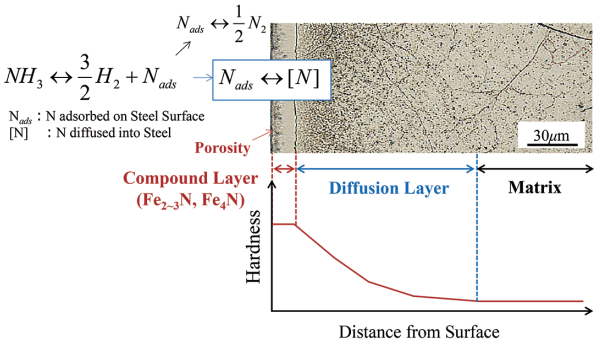

Fig. 3 Schematic diagram of microstructure and hardened layer in cross-sectional surface of nitride steel

Thus, nitrided parts consist of two hardened layers—the diffusion layer and the compound layer—and joint modification of both is considered essential to increase component strength. In what follows, we present R&D case studies focusing on each of these layers.

3. Research and Development Examples Concerning Modification of the Diffusion Layer

As noted in the preceding chapter, alloying elements influence the hardening characteristics of the diffusion layer during nitriding. The diffusion layer forms through solid-solution strengthening by nitrogen diffusing from the surface into the steel and through precipitation hardening by nitrides. In steels containing nitride-forming elements such as Cr, Al, Mo, V, and Ti, fine alloy nitrides precipitate and significantly increase hardness in the diffusion layer. However, excessive additions of these elements cause numerous alloy nitrides to precipitate near the surface, hindering diffusion of nitrogen into the steel interior and consequently reducing the effective hardened depth; this tendency is particularly strong for Al and Ti.[11)] Cr and V both form alloy nitrides and promote nitrogen diffusion into steel, thus improving both hardness and hardened depth in a balanced manner.[12, 13)]

Figure 4 shows profiles of nitrogen concentration and hardness after nitriding for a low-carbon steel equivalent to machine-structural carbon steel, a low-carbon steel with added Cr, and a low-carbon steel with added Cr and V.[14)] Additions of Cr and V, which have high affinity for nitrogen, raise the nitrogen concentration up to approximately 0.3 mm from the surface compared with the low-carbon steel without Cr or V; the hardness in this region is markedly increased

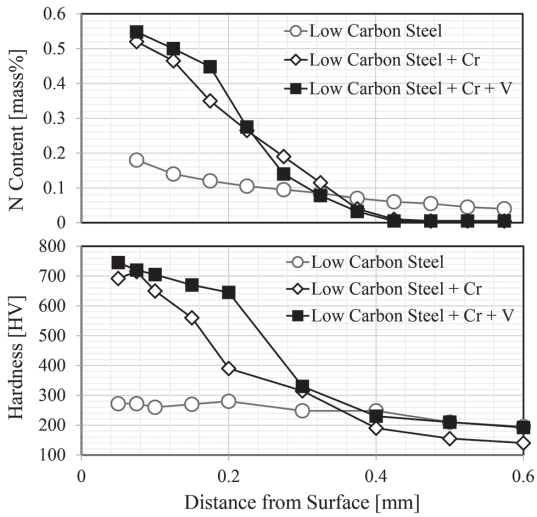

Fig. 4 Effect of Cr and V on N content and hardness distribution of diffusion layers

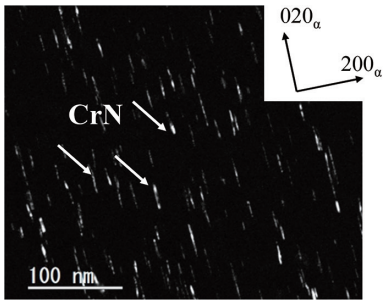

Fig. 5 Transmission electron microscopy (TEM) observations of nitrides in diffusion layer of Cr-added steel

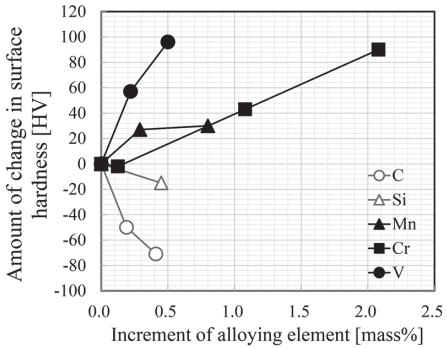

Fig. 6 Effect of alloying elements on surface hardness after nitriding

by Cr addition, and further increased hardness and a deeper hardened layer are obtained by additional V. **Figure 5** shows transmission electron microscopy (TEM) observations of nitrides precipitated in the diffusion layer when a Cr-added steel was nitrided. CrN is a plate-like nitride with a B1 crystal structure, and similar fine nitrides precipitate in steels containing Al, Ti, or V, thereby hardening the diffusion layer.[5)]

Figure 6 illustrates changes in hardness measured at 25 μm below the surface after nitriding steels based on SCr415 (0.15C-0.2Si-0.7Mn-1.1Cr [mass%]) with various additions of C, Si, Mn, Cr, and V.[8)] The hardness of the diffusion layer decreases as C content increases; moreover, the increase in hardness due to Mn is smaller than that due to Cr or V.

Factors other than steel composition also affect the nitriding response. Prior to nitriding, steels are sometimes subjected to heat treatments such as normalizing to homogenize and adjust the microstructure. Normalizing has been reported to reduce diffusion-layer hardness,[15)] with larger effects at lower normalizing temperatures.[16)] Similar tendencies are observed in steels subjected to quench-and-temper treatments or low-temperature annealing. Such treatments concentrate elements with high equilibrium partitioning to cementite (e.g., Cr) into cementite; even if cementite dissolves during nitriding, the diffusion coefficient of Cr at nitriding temperatures is small, so the dispersion state that existed in cementite tends to be preserved. When Cr precipitates as CrN from such a dispersion state, the precipitates are relatively coarse and sparse, and their contribution to hardening in the diffusion layer is reduced.[17)]

From these findings, we conclude that reducing C while adding nitride-forming elements Cr and V effectively improves the hardness profile of the diffusion layer, and that, prior to nitriding, avoiding treatments that concentrate these elements into carbides (keeping them in solid solution in the matrix) is important.

4. Research and Development Examples Concerning Modification of the Compound Layer

4.1 Modification via atmosphere-controlled nitriding

In this chapter, we present R&D examples concerning modification of the nitrogen compound layer located directly above the diffusion layer. In gas nitriding, control of the processing atmosphere using the industrial parameter called the nitriding potential (K_N) enables tailoring of the phase constitution of the compound layer. Equation (1) shows the formula for K_N.[18)]

$$K_N = \frac{P_{NH_3}}{P_{H_2}^{\frac{3}{2}}} \quad [atm^{-1/2}] \qquad (1)$$

where P_{NH_3} and P_{H_2} are the partial pressures of NH_3 and H_2 in the furnace, respectively. The state diagram of the compound layer shown as functions of K_N and temperature is referred to as the Lehrer diagram.[19)]

Figure 7 shows calculated Lehrer diagrams. In pure iron, represented by the Fe-N binary system, the stability region of the γ'-phase is wide; however, in practical steels such as machine-structural carbon or alloy steels represented by the Fe-0.2%C-N ternary system, the stability region of the ε-phase expands while that of γ' shrinks. Furthermore, in practical steels containing carbon, phase constitutions different from those of the Fe-N binary system can arise. Hiraoka et al. reported that, when nitriding JIS-SCM435, the phase of the compound layer in equilibrium with the matrix can be either ε or γ' depending on conditions.[20)] Asada et al., using Fe-Cr-0.2%C alloys, investigated the influence of Cr addition on the phase constitution of the compound layer and reported that, with increasing Cr, the phase in equilibrium with the matrix changes from γ' to predominantly ε.[21)] These differences are difficult to interpret solely from equilibrium phase diagrams and thus hinder broad application of nitrided materials with controlled compound-layer phases. It is therefore industrially important to clarify the factors affecting formation of the compound layer during nitriding and to obtain a unified mechanistic understanding.

4.2 Influence of matrix carbon content on growth of the compound layer

One reason why the phase of the compound layer in equilibrium with the matrix changes in practical steels containing carbon is considered to be decarburization from the steel surface into the atmosphere during heat treatment. Decarburization is unavoidable when heating steel and has been reported to occur during nitriding as well.[22)] Thus, the carbon concentration within the compound layer may vary over time. In this section, by studying changes in depthwise concentration profiles of alloying elements and the time evolu-

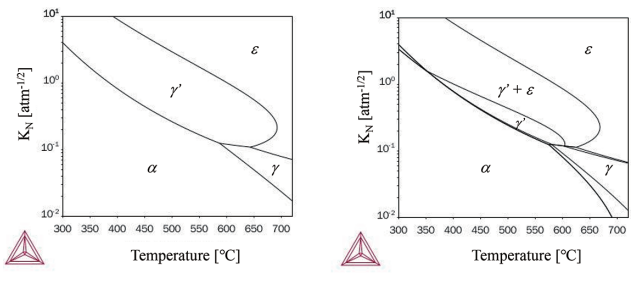

Fig. 7 Calculated Lehrer diagrams (a) Fe-N binary, (b) Fe-0.2%C-N ternary (Thermo-Calc2020, TCFe ver.10)

tion of phase constitution in the surface region when nitriding steels with different matrix carbon concentrations, we examine the mechanism by which various phase constitutions arise in Fe-C-N ternary systems.[23)]

Table 1 lists the chemical compositions of the test steels. These compositions are based on JIS-S30C, a typical machine-structural carbon steel, with C adjusted to 0, 0.3, and 0.8 mass% (hereafter C00, C30, and C80). After melting 10 kg ingots in a vacuum induction furnace, the ingots were hot-forged into round bars of 25 mm diameter. Next, normalizing was performed in accordance with JIS G 0561: C00 at 925°C, C30 at 900°C, and C80 at 870°C for 30 min. From these materials, specimens of 10×50×2 mm were machined and subjected to gas nitriding. NH_3 and H_2 gases were used for nitriding; specimens were held at 570°C for 0.5, 1.0, and 3.0 h, then cooled in oil at 80°C. The processing atmosphere was at atmospheric pressure, and gas flow rates of NH_3 and H_2 were adjusted so that K_N given by Eq. (1) was constant at the target value of 1.1 $atm^{-1/2}$. After nitriding, cross-sectional surfaces were etched with 3% nital (3% nitric acid in ethanol) and observed by optical microscopy and scanning electron microscopy (SEM). Phase identification of the compound layer was performed by electron backscatter diffraction (EBSD). Nitrogen and carbon concentrations in the compound layer were measured by glow-discharge optical emission spectrometry (GD-OES).

Figure 8 shows SEM images and EBSD phase-mapping results for the surface regions of nitrided C00, C30, and C80 steels. In C00 nitrided for 0.5 h, the compound layer consisted of ε single phase near the surface, $\varepsilon+\gamma'$ mixed phase at deeper positions, and γ' single phase adjacent to the matrix. This stacking order remained unchanged as nitriding time increased, while both γ' and ε single-phase regions grew. In C30 nitrided for 0.5 h, the top surface was ε single phase and deeper positions were $\varepsilon+\gamma'$ mixed phase. For 1.0 h and 3.0 h nitriding, the surface remained ε single phase, but the central region showed a decreasing ε fraction and became predominantly γ'. On the matrix side, γ' also predominated, though ε was more prevalent than in the central region. In C80, the compound layer was ε-dominated $\varepsilon+\gamma'$ mixed phase throughout up to 1.0 h nitriding; after 3.0 h nitriding, the structure resembled that of C30, with a higher γ' fraction near the center and a higher ε fraction near the matrix compared with C30.

Table 1 Chemical composition of experimental steel

[mass%]

	C	Si	Mn	P	S
C00	**0.00**	0.20	0.79	<0.002	0.011
C30	**0.30**	0.20	0.78	<0.002	0.010
C80	**0.82**	0.20	0.78	<0.002	0.010

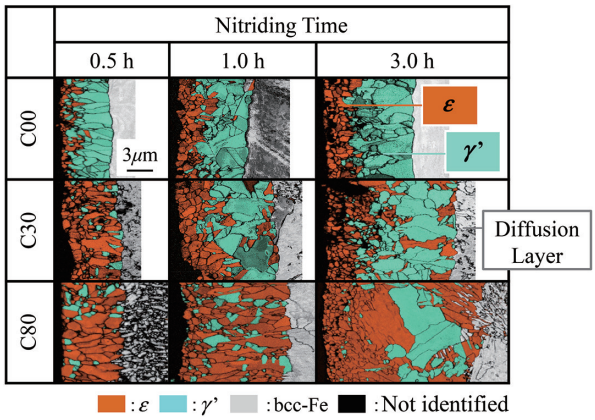

Fig. 8 Analysis results of constituent phases in compound layer by Scanning Electron Microscopy (SEM) and Electron Backscatter Diffraction (EBSD)

4.3 Correspondence between phase constitution and changes in N and C concentrations

To elucidate the reasons for the time-dependent change in phase constitution, we focused on C80, where changes were most pronounced, and investigated the time evolution of N and C concentration profiles during nitriding. The results are shown in **Fig. 9**. At all nitriding times, nitrogen concentration was highest at the outermost surface and decreased with increasing depth, dropping sharply at the depth corresponding to the compound-layer thickness. Carbon concentration exhibited a region of higher concentration within the compound layer near the matrix side than in the matrix; this is presumed to be enrichment of carbon from the matrix into the compound layer.[24)] With increasing nitriding time, the peak carbon concentration decreased. In addition, the carbon concentration at the outermost surface was lower than in the matrix, suggesting decarburization from the compound layer into the atmosphere during nitriding; the decrease grew larger with longer nitriding times.

Figure 10 shows chemical-potential profiles μ_N and μ_C calculated from measured N and C concentrations for nitrided C80. At the steel surface in contact with the nitriding atmosphere, μ_N and μ_C were nearly constant at all nitriding times; μ_N at the surface was higher than inside the steel, whereas μ_C at the surface was lower. As the compound layer thickened over time, the gradients of μ_N and μ_C along the thickness direction decreased, reducing the driving forces for N and C redistribution.

From these results, we clarified that the main factor behind time-dependent changes in the phase constitution of the compound layer is the temporal change in the depth-wise carbon concentration within the compound layer. Furthermore, the time-dependent change in carbon concentration was shown to arise from enrichment of carbon from the matrix into the compound layer and decarburization from the surface into the atmosphere, both affected by changes in the μ_C gradient along the thickness direction.

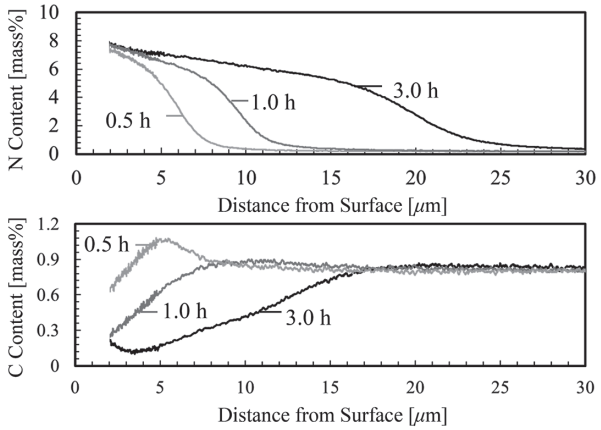

Fig. 9 Measurement results of N and C concentration distribution in surface layer of nitrided 0.8%C steel

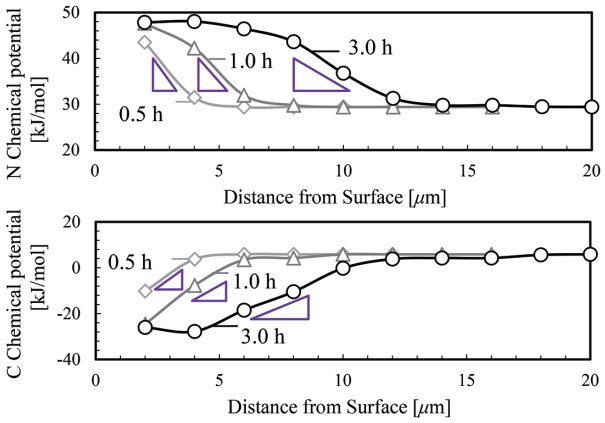

Fig. 10 Calculation results of N and C chemical potential in surface layer of nitrided 0.8%C steel (Thermo-Calc2020, TCFe ver.10)

5. Development of High-strength Steel for Atmosphere-controlled Nitriding

5.1 Overview of the developed steel

Based on the above, Nippon Steel has developed high-strength steels for nitriding. **Table 2** lists the chemical composition of a developed steel for nitriding. Compared with JIS-SCM420, the developed steel does not contain Mo, and its C and Cr contents are reduced to lower the hardness of the base material and ensure machinability, while V is added to increase the hardness of the diffusion layer and matrix through precipitation of VN and VC during nitriding. In addition, Mn is increased to obtain a predominantly bainitic matrix prior to nitriding, thereby increasing core hardness, as well as increasing the amounts of Cr and V dissolved in the matrix (solid solution). During nitriding, CrN and VN harden the diffusion layer. In the core (matrix interior), VC precipitation produces secondary hardening and suppresses matrix softening. These combined effects improve the overall hardness profile after nitriding.

5.2 Fatigue strength of the developed steel with atmosphere-controlled nitriding

In this section, we present results of evaluating tooth-root bending fatigue strength by rotating-bending tests and pitting by two-cylinder rolling tests for nitrided specimens of the developed steel. For comparison, we selected gas-carburized and quenched JIS-SCM420 widely used for automotive gears. Because achieving a compound layer rich in the more deformable γ'-phase is important for improving bending and pitting strength,[8–10,25] the nitriding atmosphere was controlled to make the fraction of γ' in the compound layer larger than that of ε.

Figure 11 compares hardness and surface microstructure before and after heat treatment for an SCM420 carburized specimen and a developed steel specimen nitrided under a controlled atmosphere. In SCM420 carburized and quenched material, intergranular oxidation layers that can serve as stress concentrators form, and non-martensitic microstructures arising from them result in relatively low surface hardness. In contrast, the developed steel after controlled nitriding achieved a compound layer predominantly consisting of γ' as intended; instead of the intergranular oxidation layer and non-martensitic microstructures observed in the carburized material, a hard, non-porous compound layer was formed.

Figure 12 shows results of rotating-bending fatigue tests and two-cylinder rolling tests. Compared with SCM420 carburized and quenched material, the developed steel after controlled nitriding exhibited 19% higher tooth-root bending fatigue strength and 21% higher pitting strength. These findings demonstrate that, by modifying both the diffusion layer and the compound layer, it is possible to enhance the strength of nitrided parts, which have traditionally had fatigue-strength limitations.

Table 2 Chemical composition of developed steel for nitriding

[mass%]

Steel	C	Si	Mn	Cr	Mo	V
JIS-SCM420	0.20	0.20	0.70	1.10	0.20	–
Developed	**0.15**	0.20	↑	↓	–	**add.**

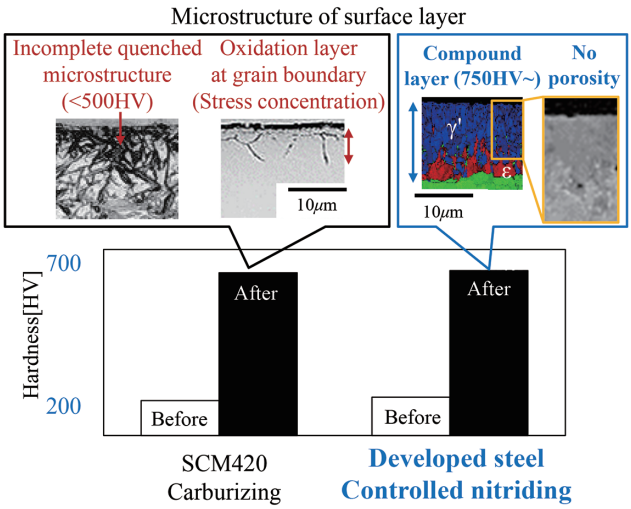

Fig. 11 Comparison of hardness and surface microstructure before and after heat treatment of SCM420 carburized specimen and developed steel controlled nitrided specimen

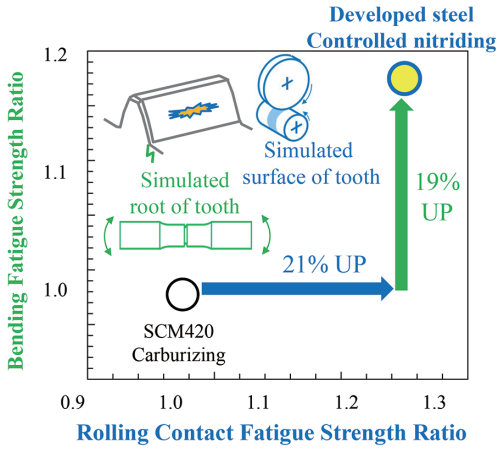

Fig. 12 Results of rotated bending fatigue test and two-cylindered rolling contact fatigue test

6. Conclusions

To expand application of nitriding to gear components, we introduced Nippon Steel's R&D case studies aimed at increasing the strength of nitrided parts. We will continue R&D not only on steel composition but also considering customer heat-treatment routes and manufacturing processes.

References

1) Ministry of Economy, Trade and Industry: Materials for the Automotive New Era Strategy Council. 2018, p. 6
2) Liedtke, D., Miyamoto, G. (supervising translator), Ishida, N. (translator): Nitriding and Soft Nitriding of Iron. AGNE Gijutsu Center, Inc., 2011, p. 9
3) Jack, D. H.: Acta Metall. 24, 137 (1976)
4) Hosmani, S. S., Schacherl, R. E., Mittemeijer, E. J.: Acta Mater. 53, 2069 (2005)
5) Miyamoto, G., Tomio, Y., Oh-ishi, K., Hono, K., Furuhara, T.: Materials Science and Technology. 27, 742 (2011)
6) Yamada, T., Kono, A.: Netsu Shori. 23, 151 (1983)
7) Takayama, T., Hinotani, S., Izumi, K., Kamata, Y., Nishida, K.: Sumitomo Metals. 48, 119 (1996)
8) Kobayashi, A., Maeda, S., Imataka, H., Gyotoku, Y., Yuya, M., Shimizu, Y., Kanayama, M.: Proceedings of the Society of Automotive Engineers of Japan, Advance Publication. 14-14, 21 (2014)
9) Takagi, S., Tonozuka, Y., Nakamura, N., Ito, T.: Tetsu-to-Hagané. 104, 594 (2018)
10) Hiraoka, Y., Ishida, A., Umezawa, O.: Netsu Shori. 57, 64 (2017)
11) Thelning, K.-E.: Steel and its heat treatment. 2nd ed. Butterworths, 1984
12) Gyotoku, Y., Imataka, H., Yuya, M., Kobayashi, A., Maeda, S.: CAMP-ISIJ. 27 (1), 504 (2014)
13) Horimoto, M., Miyanishi, K., Todo, S., Shiga, A., Imataka, H.: Nippon Seitetsu Giho. (412), 103 (2019)
14) Kiguchi, K.: The Special Steel. 71 (3), 35 (2022)
15) Egashira, M., Yuya, M., Sano, N.: CAMP-ISIJ. 20, 479 (2007)
16) Yuya, M.: CAMP-ISIJ. 25, 300 (2012)
17) Yuya, M., Egashira, M., Umehara, T.: Nippon Seitetsu Giho. (412), 116 (2019)
18) Mittemeijer, E. J., Somers, M. A. J.: Surf. Eng. 12, 152 (1996)
19) Lehrer, E.: Zeitschrift für Electrochemie. 36, 383 (1930)
20) Hiraoka, Y., Ishida, A.: Mater. Trans. 58, 993 (2017)
21) Asada, K., Kumagai, S., Watanabe, Y.: Netsu Shori. 58, 43 (2018)
22) Mittemeijer, E. J., Somers, M. A. J.: Thermochemical Surface Engineering of Steels. U.K., Woodhead Publishing, 2014, p. 352
23) Umehara, T., Yuya, M.: Netsu Shori. 59, 61 (2019)
24) Spies, H. J., Berg, H. J., Zimdars, H.: Harterei.-Techn. Mitt. 58, 189 (2003)
25) Umehara, T., Yuya, M., Tomatsu, K.: Proceedings of the 92nd Annual Meeting of The Japan Society for Heat Treatment. (2021)

Takahide UMEHARA
Senior Manager, Head of Section
Integrated Steel-Solution Research Lab.-II
Steel Research Laboratories
20-1 Shintomi, Futtsu City, Chiba Pref. 293-8511

Masato YUYA
Ph.D, Senior Manager
Intellectual Property Div.

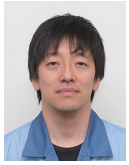

Makoto EGASHIRA
Ph.D, General Manager, Head of Dept.
Materials Characterization Research Lab.
Advanced Technology Research Laboratories